KSCE Journal of Civil Engineering (2022) 26(2):703-714
DOI 10.1007/s12205-021-1205-4

pISSN 1226-7988, eISSN 1976-3808
www.springer.com/12205

Geotechnical Engineering

Specific Dissipated Energy as a Failure Predictor for Uniform Sands under Constant Volume Cyclic Simple Shear Loading

Guillermo J. Zavala[a], **Miguel A. Pando**[b], **Youngjin Park**[c], **and Rafael Aguilar**[a]

[a]*Dept. of Engineering, Pontificia Universidad Católica del Perú, Lima 15088, Peru*
[b]*Civil, Architectural and Environmental Engineering Department, Drexel University, Philadelphia, PA 19104, USA*
[c]*Energy Production and Infrastructure Center, University of North Carolina at Charlotte, Charlotte, NC 28223, USA*

ARTICLE HISTORY

Received 5 August 2021
Accepted 26 August 2021
Published Online 27 October 2021

KEYWORDS

Dissipated energy to failure
Cyclic simple shear
Irregular cyclic loading
Cyclic behavior
Hysteresis

ABSTRACT

An experimental study was performed to investigate the dissipated energy to failure of sand samples subjected to uniform and non-uniform cyclic simple shear loading. The hypothesis evaluated was that for a given initial sample state the specific dissipated energy required to reach failure should be reasonably constant independent of the type of stress-time history used in the testing. Test samples consisted of dry Ottawa sand prepared at nine different initial states that were subjected to different stress controlled cyclic horizontal shear loading waveforms that included 15 uniform sinusoidal waves and up to 33 non-uniform loading wave forms. The experimental program presented showed that the measured cumulative dissipated specific energy to failure, defined when the double amplitude shear strain reaches 7.5%, for the different sample initial states was reasonably constant but with coefficients of variation ranging between 13 to 44%. As expected, the cumulative dissipated energy increased with increasing initial stress level and relative density. The findings support the notion that specific dissipated energy can be used as a reasonable failure predictor for uniform dry sands based on their initial state and are independent of the type of cyclic simple shear loading waveform using in the testing.

1. Introduction

Most of the early literature involving experimental studies of the cyclic behavior of sands have involved tests with uniform sinusoidal loading signals. However, nowadays with recent advances in testing equipment and control systems, it is more common to find published laboratory tests where the soil samples are subjected to more realistic loading conditions that better represent what soil layers experience during actual earthquakes (e.g., Tatsuoka and Silver, 1981; Liang et al., 1995; Xu et al., 2019). The modern geotechnical testing devices permit additional studies like the one described in this paper to help improve our understanding of the cyclic behavior of sands under more general loading conditions. As summarized in the literature review section of the paper, many experimental studies on sands have been related to the study of liquefaction of saturated sands. Most of the early studies on sand liquefaction have involved use of cyclic triaxial testing on saturated sand samples under a harmonic deviatoric stress (e.g., Seed and Lee, 1966; Silver et al., 1976; Evans, 1993; Azeiteiro et al., 2017). The early use of uniform sinusoidal load cycles required approximating the complex earthquake field loading conditions to an equivalent number of uniform load cycles (e.g., Seed et al., 1975; Annaki and Lee, 1977). As described later in the literature review section of this paper, this equivalency was initially based on achieving similar levels of cumulative damage with the equivalent uniform sinusoidal load to the cumulative damage under the more general loading demand. The more recent liquefaction literature has involved laboratory studies using cyclic simple shear tests and cyclic torsional shear under irregular load cycles. The ability to routinely perform lab tests that use more realistic and general loading types appears to have shifted the focus in liquefaction behavior research from cumulative damage towards cumulative dissipated energy (Green et al., 2000; Green and Terri, 2005; Kokusho and Tanimoto, 2021). In addition to liquefaction research, the use of specific dissipated energy may have application as a predictor of failure of sands

CORRESPONDENCE Guillermo J. Zavala ✉ gzavala@pucp.edu.pe Dept. of Engineering, Pontificia Universidad Católica del Perú, Lima 15088, Peru

under other loading types, sample states, or boundary conditions. In this paper the focus is not liquefaction of sand, but rather specific dissipated energy of dry sands subjected to constant volume simple shear load cycles of various types.

Specifically, this paper describes and summarizes the results of a comprehensive experimental program carried out to investigate whether the specific dissipated energy, i.e., the dissipated energy per unit volume of the sample, by the soil sample to reach failure is only dependent on the initial state of the sample and independent of the characteristics of the applied cyclic simple shear loading applied. To test this hypothesis, a total of 269 constant volume cyclic simple shear tests were performed on Ottawa sand samples prepared at 9 different initial states and a wide range of cyclic shear loading types. For all the tests performed the progression towards failure was carefully monitored and the computed accumulation of specific dissipated energy was tracked until failure was reached. This paper is organized into sections that include background and literature review, description of the experimental program including methodology, presentation and discussion of results, and a final section with a summary and conclusions drawn from this study.

2. Background and Literature Review

As mentioned above, the first experimental studies on liquefaction and cyclic behavior of soils involved using testing devices that primarily applied uniform sinusoidal cyclic loading. This situation required estimating an equivalency between non-uniform loading, like the type experienced by soil samples during earthquakes, and uniform sinusoidal loading. For example, the approach based on an equivalent number of uniform cycles was proposed by Seed et al. (1975) and Annaki and Lee (1977). This approach allowed evaluating the effects of different earthquake loadings on a soil tested under a simplified uniform sinusoidal loading and was based on an approach that has long been used to study fatigue of metals. For example, the Palmgren-Miner (P-M) (Palmgren, 1924; Miner, 1945) cumulative damage hypothesis was originally developed for metal fatigue and has been applied extensively in geotechnical earthquake engineering to find this equivalency between irregular and uniform loading (e.g., Seed et al., 1975; Annaki and Lee, 1977; Tatsuoka and Silver, 1981). The P-M model assumes that the damage leading to failure accumulates linearly with the number of applied cycles of loading. In the P-M model

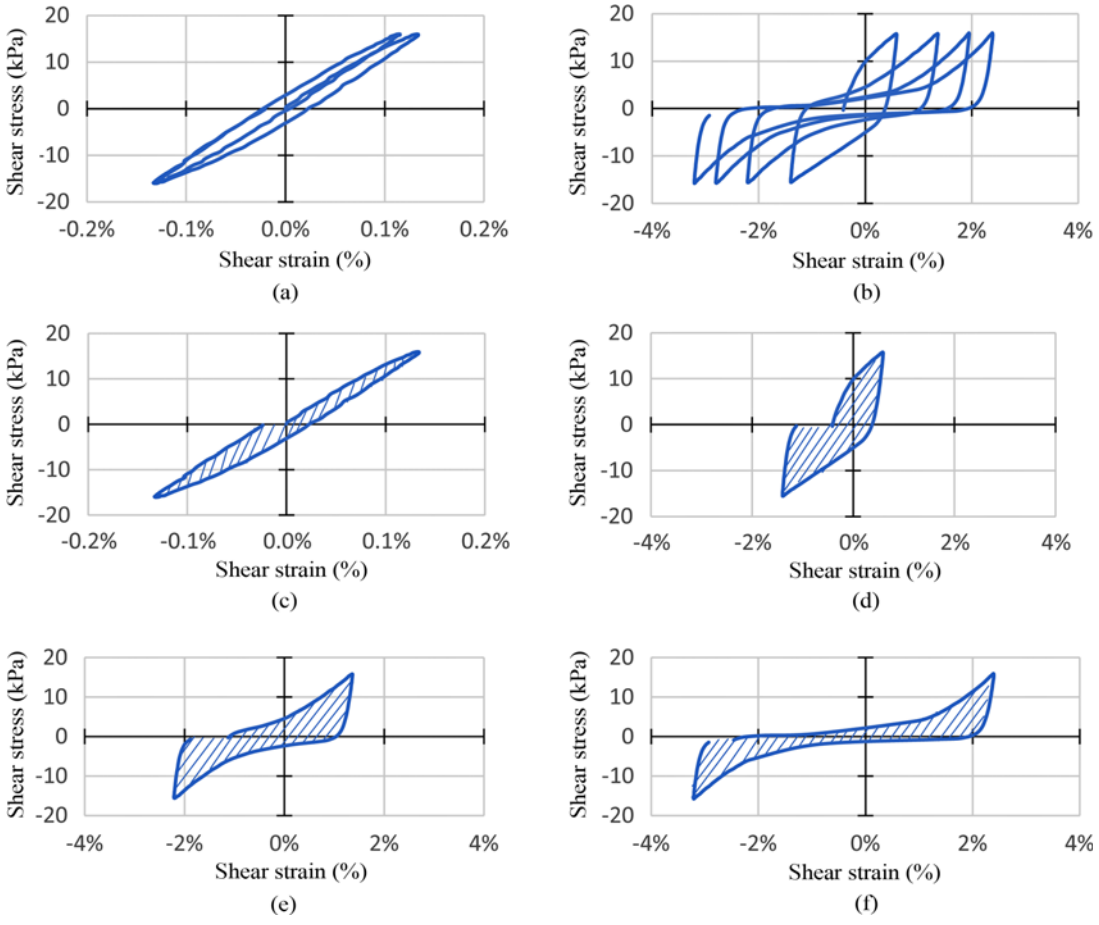

Fig. 1. Example of Different Stress-Strain Load Cycles from a Representative CSS Test from the Present Study: (a) Stress-Strain Cycles 1 and 2, (b) Stress-Strain Cycles 31 to 34, (c) Hysteresis Loop Used in the Dissipated Energy Calculation for Cycle 1, (d) Hysteresis Loop Used in the Dissipated Energy Calculation for Cycle 31, (e) Hysteresis Loop Used in the Dissipated Energy Calculation for Cycle 32, (f) Hysteresis Loop Used in the Dissipated Energy Calculation for Cycle 34

the cumulative damage is computed considering that different levels of damage will be produced in the soil subjected to a non-uniform cyclic loading. The damage produced is computed for a particular load cycle, considering that an irregular loading will contain different levels of load amplitude (e.g., different levels of cyclic stress ratio or CSR), and the soil is assumed to have reached failure when the accumulated damage computed for the different load cycles reaches a value of 100%. An equivalent number of uniform cycles at any stress level would be the value that would cause the same amount of damage to the sample. A detailed description of the P-M hypothesis can be found in Green and Terri (2005). The earlier implementation of cumulative damage based on the P-M hypothesis assumed a linear accumulation of damage. A modified non-linear cumulative damage hypothesis was proposed by Lasley (2015) and is considered a substantial improvement with respect to P-M based approaches as the computed damage is load-dependent. Cumulative damage, linear or nonlinear, remains a popular approach to estimate liquefaction failure for irregular loading demand when using experimental data that is based on application of uniform harmonic loading.

An alternative approach to the use of an equivalency between irregular loading to equivalent uniform cycles is to focus on the accumulated energy dissipated by the soil during any kind of loading demand until it reaches failure. For example, several researchers have proposed the use of energy dissipation to evaluate liquefaction potential (e.g., Ishac and Heidebrecht, 1982; Figueroa et al., 1994; Green and Terri, 2005; Kokusho and Mimori, 2015; Azeiteiro et al., 2017; Kokusho, 2017; Fardad Amini and Noorzad, 2018). The dissipated energy per unit volume of the sample, or specific dissipated energy, can be tracked during a cyclic simple shear test (CSS) by computing the area of the hysteresis loops for each shear stress versus shear strain load cycle. Examples of the dissipated energy per unit of volume for different cycles of a representative constant volume CSS test are shown in Fig. 1. The cumulative specific dissipated energy experienced by the test sample can then be computed by adding the different hysteresis loops areas in the sequence of load cycles until sample failure is reached. The stress-strain cycles from a representative CSS test shown in Fig. 1 show small energy dissipation for the initial load cycles, and larger hysteresis loops as the number of load cycles increases resulting in a faster rate of dissipated energy towards the end of the test.

Figueroa et al. (1994) and Liang et al. (1995) successfully applied the dissipated energy concept to define liquefaction potential, and validated it using undrained hollow cylinder torsional shear tests on saturated sand specimens. According to these authors, the energy per unit volume needed to induce liquefaction is not dependent on the loading form and thus can be used to evaluate the liquefaction potential of sands under general earthquake loads. Green and Terri (2005) and Lasley et al. (2016) have also used the dissipated energy concept to investigate liquefaction of sands under general loading. These authors also proposed adjustments in the approach used to measure the dissipated energy per cycle to help deal with large hysteresis loops that occur near the onset of liquefaction when significant soil softening has occurred. Kokusho (2013) reported that the cumulative dissipated energy measured on reconstituted sands tested in cyclic triaxial tests under uniform harmonic loading correlated well with pore-pressure buildup, induced strain, and onset of liquefaction. Kokusho and Kaneko (2018) confirmed this finding for similar sand samples tested using torsional simple shear tests not only under uniform harmonic loading but also under a variety of irregular load cycles. The above studies focused on liquefaction behavior of reconstituted sand samples using cyclic simple shear tests and cyclic torsional simple shear, and all support the notion that cumulative dissipated energy predicts cyclic liquefaction reasonably well irrespective of the stress-time history used in the testing. In contrast, Kokusho and Tanimoto (2021) found that the uniqueness of dissipated energy when studying the liquefaction behavior of intact soil samples in Japan, that include the inherent variability found in natural deposits, did not yield a unique correlation between cumulative energy and liquefaction when tested using cyclic triaxial tests. For intact samples and this test type, the authors found that the number of cycles to liquefaction was dependent on the level of CSR used in the test.

In summary, the existing literature involving the application of cumulative dissipated energy for the most part show that cumulative dissipated energy is a promising approach to help predict reasonably well cyclic liquefaction of reconstituted sand samples tested under cyclic simple shear and cyclic torsional shear irrespective of the stress-time history used in the testing. However more experimental studies are required to help assess the level of accuracy of the energy-based approach. The study presented herein hopes to contribute by adding to the limited number of data sets involving uniform and non-uniform load cycles and by presenting information related to the variability of the measured accumulated specific dissipated energy so the engineering community can assess the accuracy of using this parameter as a failure predictor for sands under general cyclic loading.

3. Experimental Program

The experimental program involved 269 cyclic simple shear tests conducted using an Advanced Dynamic Cyclic Simple Shear machine (ADVDCSS) manufactured by GDS Instruments. This system can independently control the vertical axial (normal) and the horizontal (shear) loads or displacements using GDS electromechanical force actuators controlled under closed loop conditions. Fig. 2 shows a general view of the ADVDCSS system, which shows the location of the vertical and horizontal actuators and the sample box. All the tests presented in this paper were run under constant volume (i.e., constant height) conditions. The samples were prepared using a cylindrical CSS sample box conformed by a stack of Teflon rings with a diameter of 70 mm and approximate sample height of 20 mm.

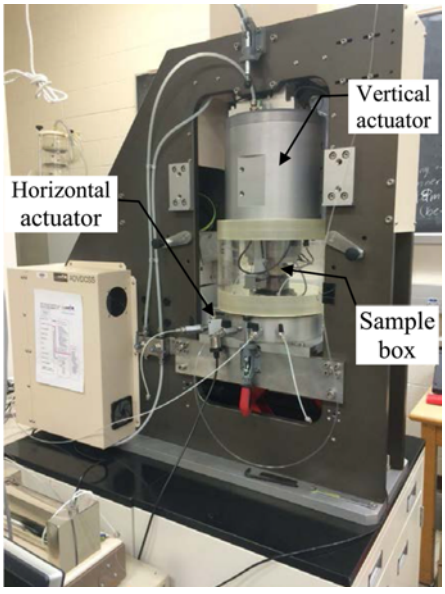

Fig. 2. Photo of the ADVDCSS System Used

3.1 Test Sand

The test sand used in this experimental program was Ottawa 20/30 silica sand. This is a uniform, poorly graded silica sand with sub-rounded to rounded grains. The mean particle size (D_{50}) of this sand is 0.71 mm, and the 20/30 designation is based on having 95% retained between the ASTM standard sieves #20 and #30. The maximum and minimum void ratios were measured using laboratory procedures in general accordance with ASTM Standard D4253 (2016) and D4254 (2016), respectively. The average maximum and minimum void ratio values obtained for the test sand were 0.644 and 0.503, respectively. The CSS tests described later were performed using dry Ottawa sand samples prepared at three different levels of relative density as shown in Table 1. This table shows the mean and standard deviation values for the 3 levels of relative density after application of the normal stress used in the CSS testing program.

The loose samples (average D_r = 28.7 %) were prepared by placing approximately 130 g of dry sand inside a 50 mm diameter open pipe that was placed vertically at the center of the CSS sample box. The pipe was then quickly pulled upwards allowing the dry sand to fill the CSS sample box in a loose condition. Next the sample top was carefully leveled, and the initial sample height measured before normal stress application. The procedure used to prepare the dense samples (average D_r = 67.5%) involved using the dry air pluviation through a glass beaker with a 5 mm steel nozzle from a height of 10 mm. The samples prepared using this technique required an approximate weight of 131.7 grams. The height of the samples at the end of the air pluviation was measured and noted. The third set of samples were very dense samples (average D_r = 93.6%) were prepared using dry tamping placed in three equal weight portions. This set of samples involved a predetermined weight of sand of 141 grams that was split into three equal portions, and each layer tamped with a flat tamper weighing 125 grams tamped until each soil layer reached a target elevation mark. In all three sample preparation methods, the sample height was measured after sample preparation (before the application of the normal stress) and after normal stress application. The reported relative densities in Table 1 and in the result section correspond to the values corrected for the final sample height after normal stress application.

The shear strength of the Ottawa sand prepared at the three relative density levels described above was measured using a Geocomp ShearTrac II direct shear device. The direct shear tests were performed in general accordance with ASTM Standard D3080 (2011). The measured peak and residual friction angles are summarized in Table 1 for the three levels of relative density considered in this study.

3.2 Cyclic Simple Shear Testing Program

The cyclic simple shear testing program involved 269 tests conducted with the ADVDCSS GDS system. The cyclic shearing phase for all tests was stress controlled and the applied normal stress was actively controlled to ensure constant sample height conditions, i.e., constant volume. The CSS test program involved 9 possible sample initial states corresponding to 3 initial relative

Table 1. Initial States of CSS Samples and Direct Shear Monotonic Shear Strength

Data Set	Number of tests	Initial State				Shear strength	
		Relative Density			Initial Stress	Peak	Residual
ID	N	State	Mean	St. Dev.	σ'_{vo} (kPa)	(ϕ'_p) (deg)	(ϕ'_r) (deg)
1	31	Loose	27.3%	3.1%	100	29°	29°
2	42		29.0%	4.1%	200		
3	46		29.7%	3.7%	400		
4	7	Dense	63.1%	4.7%	100	34°	32°
5	4		70.3%	5.2%	200		
6	4		69.0%	6.0%	400		
7	35	Very Dense	92.5%	3.1%	100	40°	32°
8	43		92.9%	3.0%	200		
9	46		95.4%	2.2%	400		

Table 2. Loading Patterns Used in This Study

Type of Cyclic Loading	Description	Parameters
Uniform	– CSR and frequency are constant in time. – 18 uniform harmonic load cycles.	– CSR values: 0.05, 0.065, 0.08, 0.09, 0.10, and 0.12. – Frequencies: 0.1, 0.5 and 1 Hz.
Non-uniform Type-1 (Alternating sine waves with different CSR and constant frequency)	– Alternating sinusoidal waves with constant frequency, but two different CSR levels that are repeated until failure.	– CSR values: combination of 0.05, 0.065, 0.08, and 0.1. – Frequencies: 0.1, 0.5 and 1 Hz.
Non-uniform Type-2 (Alternating sine waves with different frequency and constant CSR)	– Alternating sinusoidal waves with constant CSR level, but two different frequencies that are repeated until failure.	– CSR values: 0.05, 0.065, 0.08, 0.10 and 0.12. – Frequencies: combinations of 0.1 and 0.5 Hz.
Non-uniform Type-3 (Alternating sine waves with different frequency and CSR)	– Alternating sinusoidal waves with two different values of CSR and two different frequencies that are repeated until failure.	– CSR values: combination of 0.05, 0.065, 0.08, and 0.1. – Frequencies: combinations of 0.1 and 0.5 Hz.
Non-uniform Type-4 Non-uniform CSR (amplitude) - Large Spike	– Load pattern had a constant frequency. – Sequence of low of N uniform sinusoidal cycles at a low CSR value, followed by a single sine wave cycle at a high CSR value. Sequence repeated until failure reached.	– Number of low CSR uniform sine wave cycles varied from 25, 50, or 100 repetitions.

densities (loose, dense, or very dense) and 3 initial normal stresses (100, 200, or 400 kPa) (see Table 1). Samples at these 9 possible initial states were subjected to a wide range of cyclic shear loads that are listed into 5 types as described in Table 2. The first loading type listed is uniform cyclic loading. As shown in this table the test program involved 18 uniform cyclic shear loading demands that consisted of harmonic shear stresses time histories that correspond to the 6 different levels of cyclic stress ratios (CSR) and 3 frequencies used in this study. The shear stress amplitude is characterized by the CSR which is defined as

$$CSR = \tau_{cyc}/\sigma'_{vo}, \quad (1)$$

where τ_{cyc} is the amplitude of the harmonic shear stress loading time history, and σ'_{vo} is the initial normal stress level applied to the test sample before the initiation of the shearing phase.

Table 2 also lists four types of non-uniform cyclic loading demands that were used in this study for several of the initial sample states. Non-uniform load pattern Type-1 consisted of alternating sine wave cycles with a constant frequency and two different stress amplitudes (i.e., CSR values) that were alternated in a pattern repeatedly until failure. The Type-1 non-uniform load cycles involved combinations of 4 CSR values and 3 frequencies. The non-uniform load pattern Type-2 consisted in alternating sine wave cycles with a constant shear stress amplitude (i.e., CSR), but changing frequency that was alternated in a pattern repeatedly until failure. Type-2 non-uniform load cycles involved 5 different levels of CSR combined with two frequency values. The non-uniform load pattern Type-3 is similar to Types 1 and 2, but for this loading type the pattern of sine wave cycles varied both the frequency and the shear stress amplitude that was repeated until reaching failure. Type-3 non-uniform loading involved 4 CSR values, and 2 frequencies. Finally, the non-uniform load pattern Type-4 involved applying a sequence of a predetermined number of uniform sine wave cycles at a constant frequency and a low amplitude (CSR) that was then followed by a single sine wave cycle at a high amplitude (CSR) and with the same frequency as in the lower CSR sequence. This pattern of loading was repeated until failure. The large amplitude (CSR) cycle was considered a spike type loading that occurred after the application of the lower CSR sequence. The lower CSR sequences applied in this study involved three number of uniform sine wave cycles (N = 25, 50, or 100) that was then followed by the single large CSR sine wave cycle (i.e., the spike).

All 9 sets of CSS tests were carried out until failure was reached. For this experimental study failure was defined when the sample reached a 7.5% double-amplitude shear strain, which is a failure criterion commonly used in the cyclic behavior of sands literature (e.g., Finn and Vaid, 1977; Vaid and Sivathayalan, 1996; Sivathayalan and Ha, 2011; Lasley, 2015). For each CSS test results were recorded to prepare shear stress-strain plots, variation of shear strain with number of load cycles, and other summary plots (See next section). These results were used to compute the cumulative dissipated energy per unit volume for each CSS test sample until failure was reached. The cumulative dissipated energy per unit volume was computed to the last zero stress instance in the shear stress-strain cycle just prior to failure defined herein when a 7.5% double amplitude shear strain is reached (Lasley, 2015). A summary of relevant test results is provided in the next section.

4. Results

A set of representative results obtained in this study for a CSS test that used uniform load cycles are shown in Fig. 3. In this figure the CSS test results are presented using 4 plots that have matching axes in the vertical and horizontal directions and are plotted in the same scales. The graph in the upper left (Fig. 3(a)) shows the Normalized Effective Vertical Stress (NEVS), which

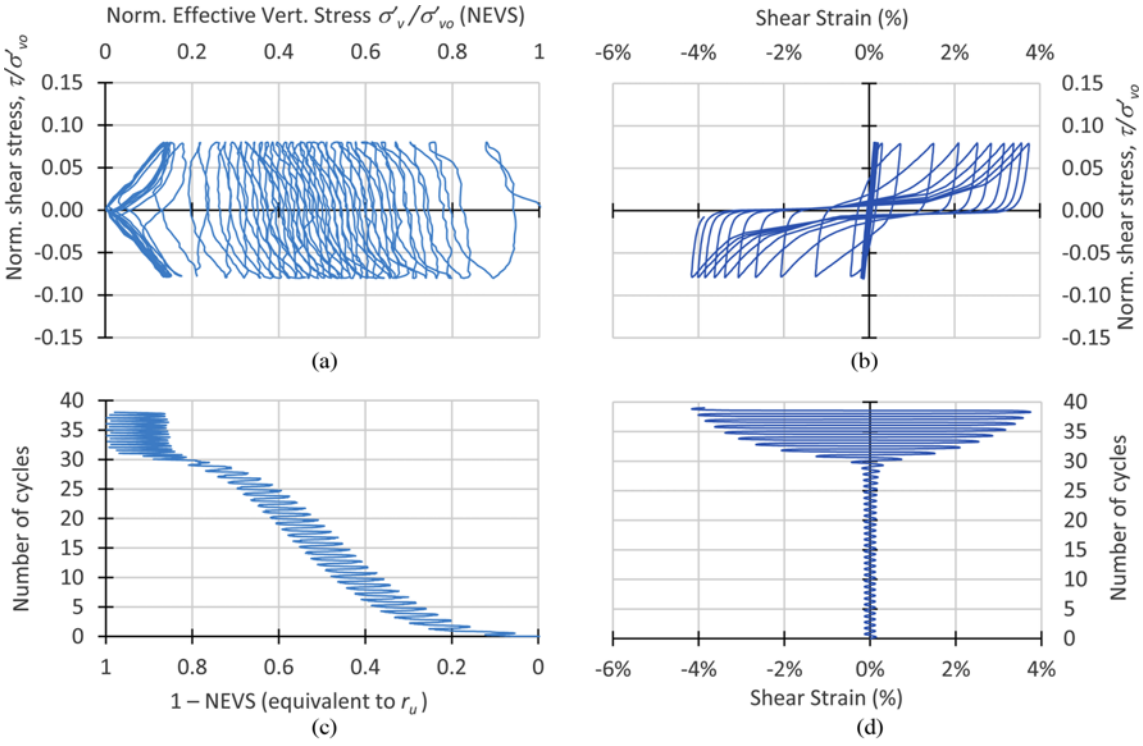

Fig. 3. Results of Uniform Constant Volume CSS Test in Very Dense Sand (σ'_{vo} = 200 kPa, CSR = 0.08, f = 0.1 Hz): (a) Norm. Effective Vert. Stress (NEVS) vs Normalized Shear Stress, (b) Shear Strain (%) vs Normalized Shear Stress, (c) 1 – NEVS vs Number of Cycles, (d) Shear Strain (%) vs Number of Cycles

is defined as the ratio between the actual vertical stress in the test and the initial vertical stress applied to the sample at the beginning of the dynamic shearing stage of the test, vs the normalized shear stress (τ/σ'_{vo}). Initially the samples have an NEVS of 1, and as the cyclic shearing progresses, the NEVS value starts to decrease until approaching a value of zero at failure. The value of NEVS decreases because the applied normal stress decreases during loading to ensure that the testing condition of constant sample height (i.e., constant volume) is maintained. This graph illustrates the progressive decrease of the vertical stress with number of applied cycles. When the sample approaches a NEVS value of 0, the shear strains start to increase dramatically which each additional cycle of load applied to the sample and the hysteresis loops and associated dissipated energy (like the ones shown in Fig. 1) tend to increase in magnitude. The graph in the upper right (Fig. 3(b)) shows the shear strain vs the normalized shear stress (τ/σ'_{vo}), illustrating the progression in size of hysteresis loops and increase of shear strain levels as the applied load cycles increase. The plot in the lower right (Fig. 3(d)) shows the variation of shear strain with number of simple shear load cycles. This graph effectively illustrates the number of cycles for which the shear strains start to increase dramatically. Closing Fig. 3, in the lower left corner, Fig. 3(c) shows the complement to NEVS, defined as 1 – NEVS, versus the number of applied load cycles. It should be noted that some authors in the liquefaction literature approximate 1-NEVS from constant volume CSS tests performed on dry samples as an equivalent pore pressure ratio (r_u) and approximate the shear strain failure as equivalent to a liquefaction failure that would be observed in an undrained CSS test performed on a saturated sample with the same initial state, under constant total normal stress. Experimental proof of this equivalency is not conclusive in the literature and there is some debate in the geotechnical community of this often-used equivalency. To avoid entering in this debate, in this paper we do not attempt to report this equivalency with undrained CSS tests, and only intended to study and report the failure behavior observed on dry sands tested under constant volume CSS tests.

The representative constant volume CSS test shown in Fig. 3 was performed on a very dense dry sand at an initial normal stress of 200 kPa, subjected to uniform harmonic cyclic stress cycles with a CSR of 0.08 and a frequency of 0.1 Hz. The progression towards failure for this sample can clearly be seen in this 4-way graph, where the shear strain starts to increase dramatically after an application of about 30 cycles and the sample finally reaches the failure criterion at Cycle 37.

Although not the focus of this paper, a close examination of the CSS test results showed that for most tests the first cycles of cyclic shear stress loading caused very small levels of shear strain that were typically less than 0.5%. As the number of cycles progressed the NEVS (normalized effective vertical stress) value gradually decreased as indicated in the representative CSS results shown in Fig. 3. For most CSS tests the shear strains rapidly increased beyond the 0.5% value when the NEVS decreased to values between 0.1 and 0.3. The upper NEVS limit of 0.3 was

observed for CSS tests involving higher CSR values, while the lower NEVS value of 0.1 was observed for CSS tests subjected to lower values of CSR, independent of the initial effective vertical stress applied to the sample or the sand initial relative density. However, CSS samples with a higher initial vertical stress and/or a higher relative density required the application of larger number of load cycles to reach these larger shear strain values beyond 0.5%. The CSS test results also showed an important difference in stress-strain behavior for loose and very dense sand when approaching the critical NEVS values of close to zero. For loose samples, the final failure, defined when a double amplitude of shear strain of 7.5% was achieved, usually occurred within 1 to 3 cycles after the NEVS value reached zero. In contrast, very dense samples did not achieve the failure criterion when the NEVS value was close to zero, as the observed shear strains increased more slowly compared to the loose samples and required 5 or more load cycles to reach failure.

The cumulative specific dissipated energy during cyclic loading was calculated for all CSS tests until failure by summing the areas inside the different hysteretic loops as described earlier and shown previously in Fig. 1. These computed cumulative specific dissipated energy values were used to test the hypothesis of this study. The hypothesis was that for a given initial sample state the specific dissipated energy required to reach failure should be reasonably constant and independent of the type of shear stress time history used in the CSS testing. As mentioned before, in this study we used 9 initial sample states defined by the relative density and stress level at the start of the application of the cyclic loading time history. The values of measured cumulative specific dissipated energy obtained for the 9 initial states considered are summarized in Table 3. The results are also summarized graphically in Figs. 4 and 5 for the loose and very dense samples, respectively. Each of these two figures show three summary plots that correspond to initial effective vertical stress values of 100, 200, and 400 kPa. The data points presented in the different summary plots reported in Figs. 4 and 5 exclude statistical outliers, which were detected using the interquartile range (IQR) method (e.g., Zwillinger and Kokoska, 1999).

The summary plots in Figs. 4 and 5 show measured values of cumulative specific dissipated energy to failure for different loading times and a given initial sample state. For example, Fig. 4(a) shows to the left the x-axis values measured for CSS tests performed using uniform load cycles. The symbol of each data point represents the frequency used and, in the corresponding x-axis labels indicate the CSR shear stress amplitude used. In a similar fashion, the data points presented towards the right end of the x-axis correspond to the different types of non-uniform loading cycles that were summarized in Table 2. It should be noted that for non-uniform loadings Type-1, Type-3, and Type-4 the labels in the x-axis show more than one CSR value depending on the characteristics of the non-uniform loading. This is not the case for non-uniform loading Type-2 where only a single CSR value is reported as this type of loading kept the CSR constant and varied only the frequency.

The research hypothesis posed in this study was that for a given initial sample state the cumulative specific dissipated energy required to reach failure should be reasonably constant and independent of the type of shear stress time history used in the CSS testing. The results in Table 3 and Figs. 4 and 5 show that the cumulative specific dissipated energy required to reach failure is reasonably constant for a given initial sample state. The results show important scatter and variability that is not uncommon in geotechnical engineering. The horizontal dashed lines shown in the summary plots of Figs. 4 and 5 correspond to the computed overall mean for all the cumulative specific dissipated energy values measured for a given initial sample state (i.e., for each of data sets). The main statistics computed for the cumulative specific dissipated energy values measured for the 9 initial states are summarized in Table 3. The level of dispersion of the measured cumulative specific dissipated energy values can be assessed from the range, standard deviation, and coefficients of variation (COV) reported in this table. For example, the coefficient of

Table 3. Cumulative Specific Dissipated Energy to Failure

Data Set	Number of tests	Initial State				Specific Dissipated Energy (kJ/m^3)					
		Relative Density			Initial Stress						
ID	N	State	Mean	St.Dev	σ'_{vo} (kPa)	Mean	St.Dev	Max	Min	COV	Descriptor*
1	31	Loose	27.3%	3.1%	100	0.2738	0.0711	0.3943	0.0916	26%	Medium
2	42		29.0%	4.1%	200	0.5664	0.1580	0.8188	0.1094	28%	Medium
3	46		29.7%	3.7%	400	1.3596	0.5942	2.4128	0.3127	44%	High
4	7	Dense	63.1%	4.7%	100	0.3403	0.1303	0.4770	0.1410	38%	High
5	4		70.3%	5.2%	200	0.8935	0.1231	1.0321	0.7335	14%	Low
6	4		69.0%	6.0%	400	2.5108	0.3266	2.9075	2.2288	13%	Low
7	35	Very Dense	92.5%	3.1%	100	0.6549	0.2169	1.2414	0.3544	33%	High
8	43		92.9%	3.0%	200	1.3214	0.4101	2.3295	0.7378	31%	High
9	46		95.4%	2.2%	400	2.9412	0.4738	3.9460	1.9418	16%	Medium

Notes: *Variability descriptor proposed by Harr (1987) based on the coefficient of variation.
St.Dev = Standard deviation; Max = Maximum; Min = Minimum; COV = Coefficient of variation.

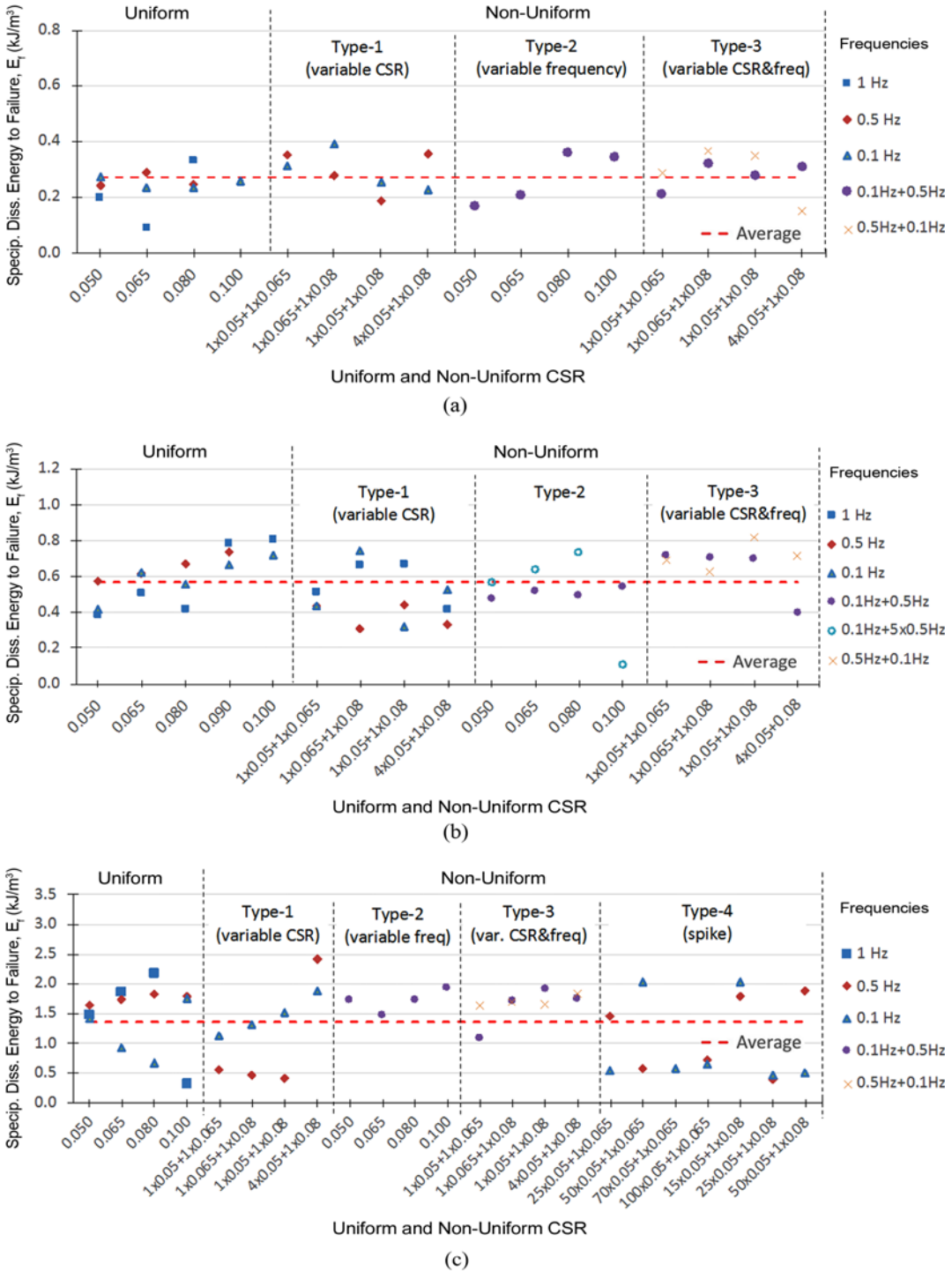

Fig. 4. Summary of Specific Dissipated Energy to Failure for Loose Sands: (a) σ'_{vo} = 100 kPa, (b) σ'_{vo} = 200 kPa, (c) σ'_{vo} = 400 kPa

variation, obtained by dividing the sample standard deviation by the sample mean, is often used as a measure of the dispersion of data. The coefficients of variation obtained for the loose, dense, and very dense relative density states ranged from 26% to 44%, 13% to 38%, and 16% to 33%, respectively. Harr (1987) provided approximate descriptors of data variability based on the values of the coefficients of variation. This author considered a "low" variability for data sets with a COV below 10%, for COV values between 15% and 30% the data variability is "moderate", and for COV values greater than 30%, a "high" variability is assigned. Based on the simplified descriptors proposed by Harr (1987), and the computed COV values in Table 3, the cumulative specific dissipated energy to failure values measured for the samples with loose and very dense states were "medium to high". In contrast, the variability was found to be between "low to high" for the data sets with a dense initial state. The larger values of COV for

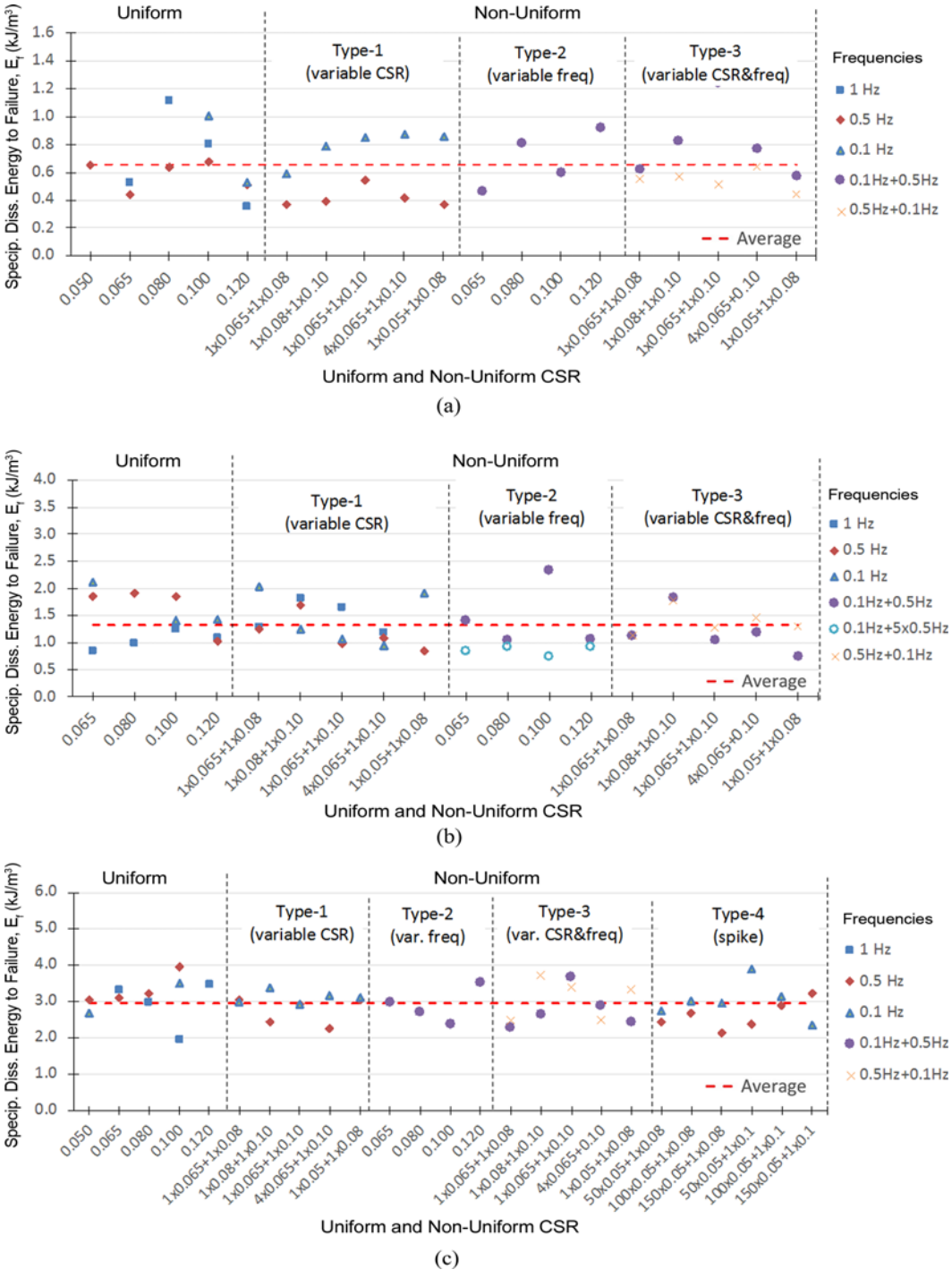

Fig. 5. Summary of Specific Dissipated Energy to Failure for Very Dense Sand: (a) σ'_{vo} = 100 kPa, (b) σ'_{vo} = 200 kPa, (c) σ'_{vo} = 400 kPa

the denser states could be associated with the larger number of cycles required to achieve the failure criterion once the NEVS = 0 condition was achieved. The stress-controlled CSS tests also showed larger hysteresis loops as the sample approached failure resulting in a large value of dissipated energy per cycle that can have a great influence in the final value of the cumulative specific dissipated energy for a test. The high influence in the computed cumulative dissipated energy to failure of the selected failure criterion and the large values of dissipated energy in the typically large hysteresis loops of the final load cycles towards failure was also highlighted by Lasley (2015).

Despite the observed levels of data variability, the measured cumulative specific dissipated energy to failure values in this experimental study were found to be reasonably constant for a given sample initial state and independent of the type of cyclic stress time history applied to the sample (see Table 2 for range of load patterns considered). Furthermore, the levels of variability observed in this study for the measured dissipated energy to

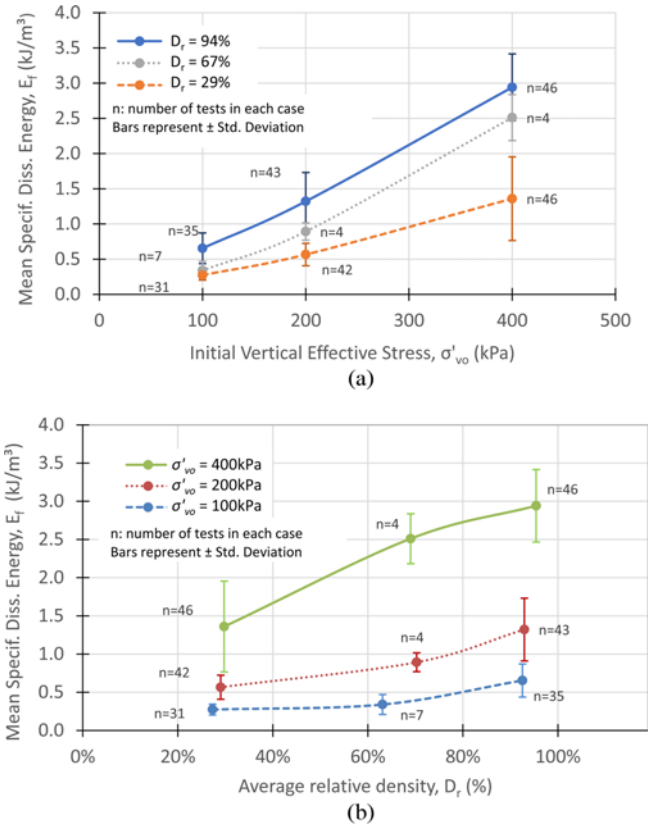

Fig. 6. Variation of the Mean Specific Dissipated Energy to Failure as a Function of: (a) Initial Vertical Effective Stress (σ'_{vo}), (b) Average Initial Relative Density (D_r)

failure were found to be comparable to the variability reported by others in the literature for experimental studies involving uniform sands tested under cyclic simple shear loading (e.g., Lasley, 2015; Kokusho and Kaneko, 2018).

The validity of the posed research hypothesis can be further investigated by plotting the mean cumulative specific dissipated energy values measured as a function of the applied initial stress level or the average initial relative density. These plots are shown in Fig. 6. Fig. 6(a) shows the variation of the measured mean cumulative specific dissipated energy to failure as a function of initial effective vertical stress level for the three levels of relative density considered. The data points shown in this plot represent the mean values, and the error bars indicate the standard deviation for each data set. This plot shows that the specific mean cumulative specific dissipated energy for a given initial relative density state increases with increasing initial effective stress level. Fig. 6(b) shows the variation of the measured mean cumulative specific dissipated energy to failure as a function of the initial relative density of the samples. This plot shows that the mean cumulative specific dissipated energy to failure for a particular initial effective vertical stress level increases with the increasing initial relative density of the sample. The two plots in Fig. 6 show the dependency of the mean cumulative specific dissipated energy to failure to the initial state of the sample that is defined by both the initial normal effective stress (σ'_{vo}) and the initial relative density (D_r) of the CSS sample and did not depend on the characteristics of the applied cyclic shear loading applied as it included a wide range of loading types. Furthermore, if we compare the relative increases of mean cumulative specific dissipated energy to failure in both plots, the changes were larger for an increase in the initial effective vertical stress compared to an increase of the initial relative density of the samples. However, this observation is specific to the initial states considered in this experimental study where the range of relative densities considered did not cover the full range of values for the test sand used in the study. Finally, even though Fig. 6 shows that the mean cumulative specific dissipated energy to failure depends on the initial sample state and not on the characteristics of the applied cyclic shear loading time history the error bars shown in Fig. 6 reveal an important variability of the mean cumulative specific dissipated energy to failure.

5. Conclusions

A test program was designed and performed to evaluate the research hypothesis that the cumulative specific dissipated energy required to reach failure measured in CSS tests should be reasonably constant for a given initial sample state defined by the initial relative density and stress level and independent of the type of stress-time history applied to the test sample. A total of 269 constant volume cyclic simple shear (CSS) tests were conducted under uniform and non-uniform shearing loading applied to dry Ottawa sand samples prepared at nine initial stress states that corresponded to three relative density levels (loose, dense, and very dense), and three initial vertical effective stresses levels (100, 200, and 400 kPa). The test program involved uniform and non-uniform cyclic shear time histories with different frequencies, amplitudes, and patterns as described in Table 2. The experimental program presented showed that the measured cumulative dissipated specific energy to failure, defined when the double amplitude shear strain reaches 7.5%, for the different sample initial states was reasonably constant and independent of the type of loading applied to the sample. However, the test results showed coefficients of variation ranging between 13 to 44% indicating significant variability of the measured values of cumulative dissipated specific energy to failure. The higher values of COV were observed for the CSS tests involving very dense samples where it was observed that more load cycles were required at NEVS = 0 state in order to achieve the specified failure criterion. This larger number of load cycles also had large hysteresis loops thus having a large influence in the final value of the measured cumulative specific dissipated energy. The level of variability observed in the measured dissipated energy to failure was to be comparable to the variability reported by others in the literature for experimental studies involving uniform sands tested under cyclic simple shear loading.

Despite the significant levels of data variability observed, the measured values of cumulative specific dissipated energy to failure were found to be reasonably constant for a given sample

initial state and independent of the type of cyclic stress time history applied to the sample. The mean cumulative specific dissipated energy was found to increase with increasing initial stress level and relative density. The findings support the notion that specific dissipated energy can be used as a reasonable failure predictor for uniform dry sands based on their initial state and are independent of the type of cyclic simple shear loading waveform using in the testing.

In conclusion, this experimental study helped evaluate and validate the research hypothesis that for a given initial sample state the cumulative specific dissipated energy required to reach failure of a uniform, dry, sand sample tested under stress-controlled, constant volume CSS testing should be reasonably constant and independent of the type of stress-time history used in the testing. However, the measured values of cumulative specific dissipated energy required to reach failure were found to have some important variability that may be related to inherent variability of geotechnical parameters even under relatively well controlled conditions available in laboratory studies like the present one. The findings reported herein need to be validated for other testing conditions including truly undrained CSS tests, cyclic triaxial, and for non-uniform samples such as undisturbed, intact samples from the field.

Acknowledgments

The first author would like to thank the Pontificia Universidad Católica del Perú for the funding provided to spend a sabbatical year and two summer periods at UNC Charlotte as a visiting scholar where the bulk of the experimental tests were performed. This author also thanks the CEE department of UNC Charlotte and the second author for providing office space, and access to the testing and computing facilities during his visiting scholar periods.

ORCID

Guillermo J. Zavala https://orcid.org/0000-0002-2077-5001
Miguel A. Pando https://orcid.org/0000-0001-9940-7887
Youngjin Park https://orcid.org/0000-0001-9942-7618
Rafael Aguilar https://orcid.org/0000-0002-8175-8950

References

Annaki M, Lee KL (1977) Equivalent uniform cycle concept for soil dynamics. *Journal of the Geotechnical Engineering Division-ASCE* 103(GT6):549-564, DOI: 10.1061/AJGEB6.0000436

ASTM D3080 (2011) Standard test method for direct shear test of soils under consolidated drained conditions. ASTM D3080, ASTM International, West Conshohocken, PA, USA, DOI: 10.1520/D3080_D3080M-11

ASTM D4253 (2016) Standard test methods for maximum index density and unit weight of soils using a vibratory table. ASTM D4253, ASTM International, West Conshohocken, PA, USA, DOI: 10.1520/D4253-16E01

ASTM D4254 (2016) Standard test methods for minimum index density and unit weight of soils and calculation of relative density. ASTM D4254, ASTM International, West Conshohocken, PA, USA, DOI: 10.1520/D4254-16

Azeiteiro RJN, Coelho PALF, Taborda DMG, Grazina JCD (2017) Energy-based evaluation of liquefaction potential under non-uniform cyclic loading. *Soil Dynamics and Earthquake Engineering* 92:650-665, DOI: 10.1016/j.soildyn.2016.11.005

Evans MD (1993) Liquefaction and dynamic properties of gravelly soils. Eco-architecture 2022, July 12-14, Lisbon, Portugal

Fardad Amini P, Noorzad R (2018) Energy-based evaluation of liquefaction of fiber-reinforced sand using cyclic triaxial testing. *Soil Dynamics and Earthquake Engineering* 104:45-53, DOI: 10.1016/j.soildyn.2017.09.026

Figueroa JL, Saada AS, Liang LQ, Dahisaria NM (1994) Evaluation of soil liquefaction by energy principles. *Journal of Geotechnical Engineering-ASCE* 120(9):155-1569, DOI: 10.1061/(ASCE)0733-9410(1994)120:9(1554)

Finn WDL, Vaid YP (1977) Liquefaction potential from drained constant volume cyclic simple shear tests. *Proceedings of 6th World Conference on Earthquake Engineering* 3:2157-2162

Green RA, Mitchell JK, Polito CP (2000) An energy-based excess pore pressure generation model for cohesionless soils. Proceedings of the John Booker memorial symposium, November 16-17, Balkema, Rotterdam, Netherlands

Green RA, Terri GA (2005) Number of equivalent cycles concept for liquefaction evaluations - Revisited. *Journal of Geotechnical and Geoenvironmental Engineering-ASCE* 131(4):477-488, DOI: 10.1061/(ASCE)1090-0241(2005)131:4(477)

Harr ME (1987) Reliability-based design in civil engineering. McGraw-Hill, New York, NY, USA

Ishac MF, Heidebrecht AC (1982) Energy dissipation and seismic liquefaction in sands. *Earthquake Engineering and Structural Dynamics* 10(1):59-68, DOI: 10.1002/eqe.4290100105

Kokusho T (2013) Liquefaction potential evaluation: Energy-based method versus stress-based method. *Canadian Geotechnical Journal* 50(10):1088-1099, DOI: 10.1139/cgj-2012-0456

Kokusho T (2017) Liquefaction potential evaluations by energy-based method and stress-based method for various ground motions: Supplement. *Soil Dynamics and Earthquake Engineering* 95:40-47, DOI: 10.1016/j.soildyn.2017.01.033

Kokusho T, Kaneko Y (2018) Energy evaluation for liquefaction induced strain of loose sands by harmonic and irregular loading tests. *Soil Dynamics and Earthquake Engineering* 114:362-377, DOI: 10.1016/j.soildyn.2018.07.012

Kokusho T, Mimori Y (2015) Liquefaction potential evaluations by energy-based method and stress-based method for various ground motions. *Soil Dynamics and Earthquake Engineering* 75:130-146, DOI: 10.1016/j.soildyn.2015.04.002

Kokusho T, Tanimoto, S (2021) Energy capacity versus liquefaction strength investigated by cyclic triaxial tests on intact soils. *Journal of Geotechnical and Geoenvironmental Engineering-ASCE* 147(4):04021006, DOI: 10.1061/(asce)gt.1943-5606.0002484

Lasley SJ (2015) Application of fatigue theories to seismic compression estimation and the evaluation of liquefaction potential. PhD Thesis, Virginia Tech, Blacksburg, VA, USA

Lasley SJ, Green RA, Rodriguez-Marek A (2016) Number of equivalent stress cycles for liquefaction evaluations in active tectonic and stable continental regimes. *Journal of Geotechnical and Geoenvironmental Engineering-ASCE* 143(4):04016116, DOI: 10.1061/(ASCE)GT.1943-

5606.0001629

Liang L, Figueroa JL, Saada AS (1995) Liquefaction under random loading: Unit energy approach. *Journal of Geotechnical Engineering-ASCE* 121(11):776-781, DOI: 10.1061/(ASCE)0733-9410(1995)121:11(776)

Miner MA (1945) Cumulative damage in fatigue. *Journal of Applied Mechanics* 12(3):A159-A164

Palmgren A (1924) Die lebensdauer von kugellagern. *Zeitschrift Des Vereins Deutscher Ingenieure* 68(14):339-341

Seed HB, Idriss IM, Makdisi F, Banerjee N (1975) Representation of irregular time histories by equivalent uniform stress in liquefaction analysis. Report No. EERC 75-29, Earthquake Engineering Research Center, University of California, Berkeley, Berkeley, CA, USA

Seed HB, Lee KL (1966) Liquefaction of saturated sands during cyclic loading. *Journal of the Soil Mechanics and Foundation Division-ASCE* 92(6):105-134, DOI: 10.1061/JSFEAQ.0000956

Silver ML, Chan CK, Ladd RS, Lee KL, Tiedemann DA, Townsend FC, Valera JE, Wilson JH (1976) Cyclic triaxial strength of standard test sand. *Journal of the Geotechnical Engineering Division-ASCE* 102(5):511-523, DOI: 10.1061/AJGEB6.0000272

Sivathayalan S, Ha D (2011) Effect of static shear stress on the cyclic resistance of sands in simple shear loading. *Canadian Geotechnical Journal* 48(10):1471-1484, DOI: 10.1139/T11-056

Tatsuoka F, Silver M (1981) Undrained stress-strain behavior of sand under irregular loading. *Soils and Foundations* 21(1):51-66, DOI: 10.3208/sandf1972.21.51

Vaid YP, Sivathayalan S (1996) Static and cyclic liquefaction potential of Fraser Delta sand in simple shear and triaxial tests. *Canadian Geotechnical Journal* 33(2):281-289, DOI: 10.1139/t96-007

Xu DS, Liu HB, Rui R, Gao Y (2019) Cyclic and postcyclic simple shear behavior of binary sand-gravel mixtures with various gravel contents. *Soil Dynamics and Earthquake Engineering* 123:230-241, DOI: 10.1016/j.soildyn.2019.04.030

Zwillinger D, Kokosk S (1999) CRC Standard probability and statistics tables and formulae. CRC Press, Boca Raton, FL, USA, DOI: 10.1201/9781420050264